A Wide Angle Airborne or Spaceborne Laser Ranging Instrumentation for Millimeter Accuracy Subsidence Measurements

O. BOCK and M. KASSER
Ecole Supérieure des Géomètres & Topographes, 18 allée Jean Rostand, 91025 EVRY Cedex, France

Ch. THOM
Institut Géographique National, Laboratoire d'Optoélectronique et de Microinformatique, 2 avenue Pasteur, BP 68, 94160 Saint Mandé, France.

I. INTRODUCTION

A wide-angle airborne laser ranging system is under investigation at IGN [i, ii]. This system is intended to achieve a new geodesy technique, based on aerial multilateration. Extension to a spaceborne system is also considered. The technique should have the capability of detecting height displacements of ground-based benchmarks with sub-millimeter accuracy in a very short time (a few hours). It would be particularly adapted to the daily monitoring of a network of typically 100 benchmarks, extending over an area of 10 by 10 km. For instance, it would be adequate for estimating surface effects induced from fluid withdrawal or solid extraction [iii]. But it can be extended to periodic monitoring of more general geophysical processes where a millimeter accuracy of the vertical component is required, e.g., tectonics, volcanology, and geology. Assuming that some benchmarks are fixed, i.e., that they are far away from the deformation area, only relative locations are to be considered since one is interested in displacements not locations.

Airborne or spaceborne laser ranging systems, with the ranging system onboard, appear as attractive solutions for monitoring large networks of ground-based retroreflectors. Several such systems have been studied during the last fifteen years [iv, v, vi]. But the use of multi-beam, servo-controlled, pointing systems made them rather complicated and they were, in a first time, transformed into single narrow beam systems and, finally, abandoned. Using a wide-angle beam simplifies considerably the instrumentation while needing a proper signal processing, in order to identify which reflectors are measured. In order to assess the accuracy of such a system, we have developed a first instrument made several terrestrial experiments.

In section 2 of this paper, we describe the principle of wide-angle aerial and spatial multilateration. Such techniques are based on simultaneous distance measurements, achieved, in our case by the use of a wide angle laser beam. The instrumentation and its associated signal processing is presented in section 3. In section 4 we analyze the main error sources : atmospheric effects, laser effects, and effects from the detection electronics (signal-strength related biases, electrical noise, and temporal jitters). In section 5 we present experimental results, obtained from three different terrestrial experiments. Finally, in section 6 we propose an optimization of the current instrumentation, to fulfill the requirements for airborne and also spaceborne configurations.

II. PRINCIPLE OF WIDE-ANGLE AERIAL AND SPATIAL MULTILATERATION

The aerial or spatial multilateration technique is based on range measurements, to a network of ground based benchmatrks, performed from an airborne or spaceborne platform

(Figure 1). By using an inverse method, benchmarks can then be positioned, with an accuracy depending only on the accuracy and number of measurements and the geometrical configuration. Typically, the single-shot ranging accuracy is a few centimeters, and requires negligible biases.

We investigated this technique a few years ago, by a numerical simulation approach, based on the assumption that an ad hoc instrument could be developed to fulfill these requirements. We found that the objective of a vertical precision of 1 mm could be achieved, using a least-squares adjustment method, with some requirements on measurements. A priori locations of the aircraft and the benchmarks have to be known within a few decimeters. This requirement is not critical because it is used only as a first trial of a few iterations. On the other hand, the accuracy of relative distances and the number of measurements are critical. They must respectively be, for example, a few centimeters and a few thousands per retroreflector. The a priori locations are easily achievable by GPS techniques, e.g., Differential-Trajectography for the aircraft, and Rapid-Static for the ground based benchmarks. Note that the complete network survey for a priori locations has only to be performed once, before the first aerial survey. Posterior surveys can simply use the previous results.

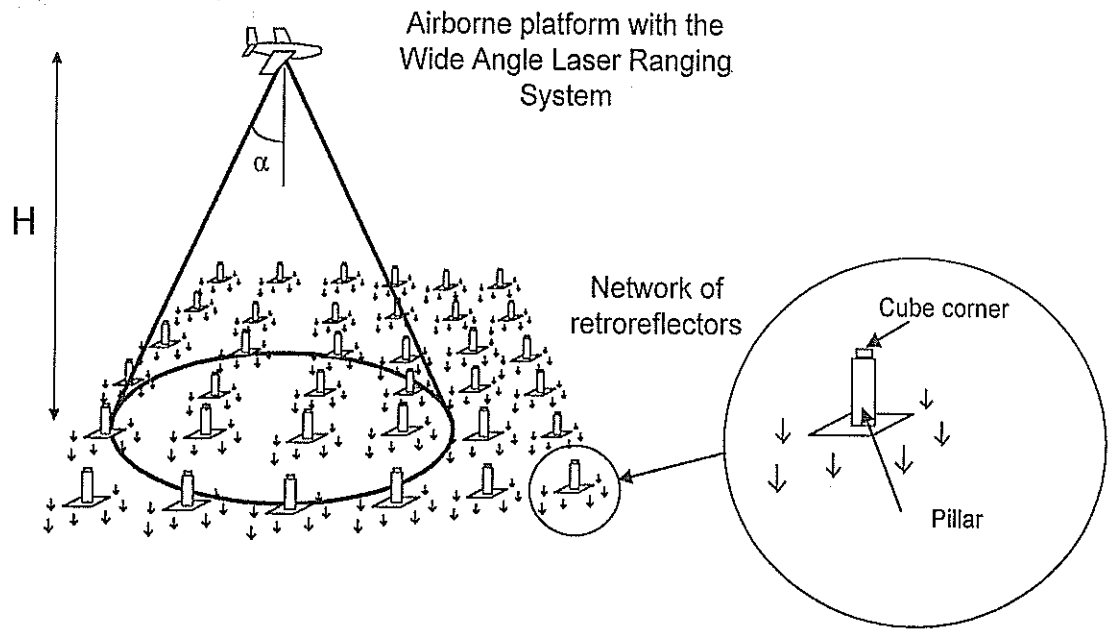

Figure 1: View of a typical airborne configuration, over a ground-based retroreflector network.

The use of a widely diverging laser beam (± 15 ° around nadir), illuminating the network of ground-based optical cube corners, seems a good solution to this problem. For one pulse transmitted by the laser, several echoes (typically ten) are retroreflected. By estimating precisely their times-of-flight and correcting for the mean refraction effect we achieve simultaneous range measurements and create strong constraints on both the coordinates of the laser source with respect to the network of reflectors, and between the coordinates of the reflectors. Note also that, the more the laser beam is divergent, the best is the horizontal accuracy of the positioned benchmarks. But since we are mostly interested in the vertical component, the range measurements are preferably done in a moderate field with around nadir. Atmospheric refraction effects are thus not critical to correct. By a proper modeling of both direct and inverse problems, one can also add other unknowns to the fundamental model, like a range bias fluctuating from shot to shot. By taking into account such a range bias, one has only to estimate arrival times of the laser echoes. The associated ranges are then called pseudo-distances, as in GPS where the transmitter

and receiver clocks are not synchronized. Relative pseudo-distances become then fundamental observations. Modeling the range bias has two interesting consequences. Firstly, it relaxes the constraints on refraction index correction as only differential variations need to be corrected. Secondly, it allows to record the detected signal only during the time window where echoes are expected. The amount of static memory of the recorder (digital oscilloscope, cf. next section) can thus be reduced.

III. INSTRUMENTATION AND SIGNAL PROCESSING

A. Instrumentation

A block diagram of the wide angle laser ranging system is illustrated in Figure 2. The mode-locked Nd:YAG laser transmitter (modified Quantel, from the Mobile Satellite Laser Station, Observatoire de la Côte d'Azur, Grasse, France) is based on a stable cavity with uniform reflectivity mirrors, aperture for TEM_{00} mode selection, passive Q-switch (saturable absorber) and active mode-locking (acousto-optic modulation). Mode-locking produces a train of 100 psec pulses in an average waveform of 70 nsec (FWHM), of which one pulse is extracted and amplified up to 100 mJ by a double-pass Nd:YAG amplifier. The pulse repetition frequency is 10 Hz.

The wide-angle beam is produced by whether a diverging lens or a ground glass plate, and is typically 15° at half-angle. But, in order to reduce irradiance fluctuations produced by speckle patterns, a diverging lens is preferred [vii]. For each laser shot, multiple echoes, arising from the network of retroreflectors, are detected and their waveforms are recorded. The photodetector is composed of a large area (1 cm^2) PIN photodiode (EG&G, YAG 444). The long transit-time of the photodiode (about 6 nsec), combined with a high transimpedance amplifier (3000 V/A gain, 50 MHz bandwidth), produces electrical response pulses of typically 13 nsec (FWHM), with a 4 nsec leading edge. The electrical signal is sampled by a digital oscilloscope (Lecroy 7200), with a 1 nsec period, and stored, whether in central memory of the oscilloscope or on the hard-drive of a host computer (Fieldworks 7500, PC) in real-time by GPIB. Note that the hardware of our system is much simpler than earlier proposed airborne and spaceborne systems [iv, v, vi], and also than current SLR systems [viii]. In return, the digitized signal has to be processed properly to retrieve the times-of-flight of laser pulses.

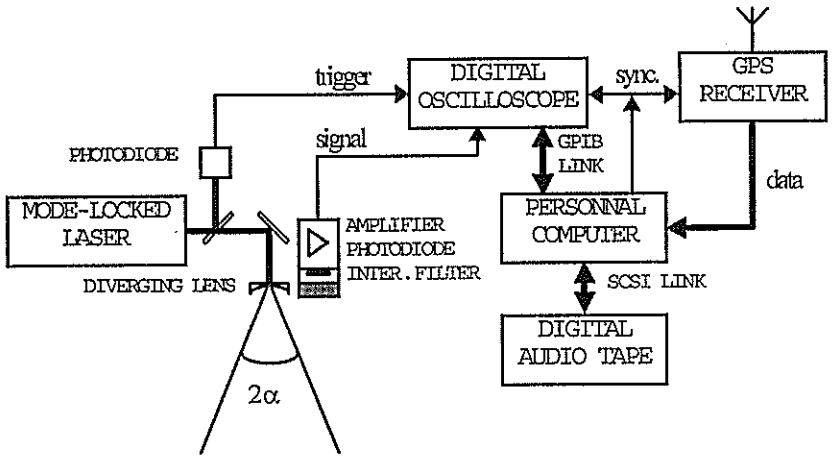

Figure 2 : Block diagram of the wide-angle airborne laser ranging instrument. A fixed GPS receiver (not shown) is also required at a ground station for differential trajectography.

B. Signal processing

The signal processing is composed of two steps. Firstly, measured echoes have to be properly identified, i.e., detected pulses have to be assigned reflector numbers. Therefore, the range bias is roughly estimated by correlating the measured signal with a Dirac comb composed of delta-functions at the approximate arrival times, calculated from a priori locations. The resulting range bias is accurate within one sampling interval, i.e., 1 nsec (15 cm), which is far enough for detecting 13 nsec FWHM pulses. Remember that the residual range bias is accurately estimated during the global inversion. Secondly, times of arrival of the detected pulses are estimated with an accuracy of, say, 100 psec (15 mm). To achieve this, one can implement either sub-optimum methods, or optimum methods, e.g., minimum mean-square error and maximum likelihood methods. We analyzed several ones, such as leading-edge threshold detection, center-of-gravity, cross-correlation and deconvolution. The first two belong to the sub-optimum estimator class, while the last two are two implementations of the same optimum method. Table 1 compares the theoretical precision of these methods.

Estimation method	Leading edge	Center-of-gravity	Cross-correlation
Single-shot accuracy	42 psec (6.3 mm)	29 psec (4.3 mm)	23 psec (3.4 mm)

Table 1 : Theoretical single-shot precision, i.e., standard deviation or estimation error in presence of additive noise, of several time-of-arrival estimators. Signal and noise characteristics are representative of the current instrumentation, assuming an electrical SNR of 100.

When combining the approximate range bias, i.e., the time of departure of the laser pulse, and the estimated times of arrival of the reflected pulses, one has a set of simultaneous "pseudo" times-of-flight. Here again, "pseudo" refers to the fact that only relative times-of-flight are known with the proper accuracy. When converting these times to distances, with the help of an atmospheric refraction model, e.g. [ix], one gets a set of simultaneous pseudo-distances. Therefore, we consider only relative distances.

Cross-correlation is an efficient pseudo-range estimator for individual pulses. But in operational configurations several pulses are reflected simultaneously. Pulse-superimposition, when reflectors are close in distance, produce then biases because pulse shapes are altered. In order to take into account the mutual effect of pulses, it is necessary to estimate simultaneously all the echoes in the oscilloscope trace. Therefore, we implemented a deconvolution method, fitting pulses of a synthetic trace on every measured trace by a least-squares adjustment. The reference pulses of the synthetic trace must be close, in their waveforms, to the real pulses. Therefore, we use an average measured pulse. Note that this method is, on a mathematical point of view, equivalent to the cross-correlation, with a reference function equal to the average measured pulse. In a second step we perform a sorting of the ranges estimated, rejecting all ranges closer than 4 m to another range. In this way we avoid to use estimations from pulses which may be affected by superimposition effects or even which may be wrongly affected a reflector number.

IV. Error sources in wide angle laser ranging

A. Atmospheric effects

The first error source stems from atmospheric refraction.Since we are interested in relative distances, only differential refraction effects have to be corrected, i.e., stemming from the part of atmosphere between the reflectors. When using local meteorological measurements, one is able to correct for this effect with an accuracy of a few mm with a spherical shell model [ix]. In a typical application, these parameters are necessary in order to correct for tropospheric effects of

GPS measurements, at the reference, ground based, station and in the aircraft. It is thus necessary to relate the atmospheric parameters at the reflectors of the network to these meteorological measurements. This can be done with the help of basic thermodynamics. Deviations of local parameters from this model, especially in the boundary layer, should lead to biases lower than 1 mm. On the other hand, turbulence produces also path length fluctuations. The strength of this effect can be evaluated by the path length structure function [x]. It should remain below the millimeter level both in the case of the terrestrial experiments presented in section 5 and in the case of a typical airborne experiment. In the general case, refraction effects can thus be neglected.

A second effect, induced by atmospheric turbulence, is irradiance fluctuations, or scintillation. Phase perturbations of the propagating optical wave induce interference effects and, therefore, intensity, phase and angle-of-arrival fluctuations at a point receiver. In weak turbulence regime, intensity statistics are governed by a log-normal probability density function (pdf) [xi], whereas in strong regime, the pdf become rather exponential [xii]. We can therefore expect, in aerial, and even more in spatial, configurations near unity scintillation contrasts. The main effect of these fluctuations is a reduction of the number of simultaneous measurements above a fixed SNR threshold. The impact of the remaining atmospheric induced scintillation, on the constraints created by the measured pseudo-distances on the multilateration problem, is one of the next effects to be analyzed. A statistical analysis of this phenomenon would be useful to optimize instrumental parameters, such as beam divergence, pulse repetition frequency, and aerial survey duration or number of satellite passes.

B. Laser beam effects

Wavefront distortions in laser beams have been well known to the SLR community, because they are among the most limiting phenomena at the instrumentation [xiii]. Biases up to a few nanoseconds have been reported in Q-switched lasers [xiii]. We have also investigated two different laser transmitters and measured biases reaching half the pulsewidth at the edge of the beam [ii]. The first laser was an unstable cavity resonator, with super-gaussian mirrors (Quantel, Brillant), transmitting a 4 nsec, 350 mJ pulse. The second laser was the mode-locked laser, described in section 3. We showed that our mode-locked laser produces biases, in the near-field, of about 100 psec (15 mm) at the edge of the beam ($1/e^2$ intensity), or 50 psec (7.5 mm) at FWHM, while for the unstable cavity laser, biases reach 2 nsec at the edge [ii]. Mode-locked lasers have the advantage of producing a smooth temporal waveform pulse and low far-field angular biases thanks to the transverse mode stability achieved by the long build-up of the beam. Nevertheless, there exist some other means of achieving picosecond laser pulses, with consequently low wavefront distortion, such as pulse compression techniques, e.g., backward Stimulated Brillouin Scattering [xiv]. But such devices have not yet been evaluated.

C. Signal strength related biases in the detection stage

The second, deterministic, error source is a temporal bias depending on the signal magnitude, stemming from both the photodiode and the amplifier. As the signal magnitude fluctuates, this effect increases the bias and the standard deviation of range measurements. A characterization of the detection stage revealed this effect was present predominantly in the amplifier but was not significant in the photodiode. A linear relationship, with a slope of 0.5 m/V, has been reported [vii]. It can thus be corrected on individual range measurements, knowing their amplitude. Without correction, biases of almost 20 cm may arise, whereas corrected data exhibit a gaussian scatter of a few cm standard deviation [vii].

D. Electrical noise in the detection stage

Electrical noise in the detection stage is mainly composed of additive Gaussian noise from the photodetector, amplifier and oscilloscope. The predominant noise in the photodiode is shot-

noise stemming from the received laser pulses, solar background illumination, and dark current. The solar irradiance is reduced by an interference filter of large bandwidth (20 nm at 1.064 μm), allowing transmission of the wide angle beams. This current is, with the dark current, generally negligible with respect to the signal photocurrent. Thus, only shot-noise produced by the laser pulses has to be considered. The total shot-noise is about 70 μV for a 100 mV signal magnitude at the output of the amplifier. Electrical noise in the amplifier is mainly produced by active components, such as bipolar transistors. It reaches 260 μV rms for a 95 MHz bandwidth. The oscilloscope produces electrical noise and quantization effects, though the second effect is negligible. We measured typical values of 230 μV, rms, at 5 mV/div.

We compared photodiode shot-noise, amplifier noise and oscilloscope noise, for caliber ranging from 5 mV/div. to 500 mV/div., and assuming the detected signal is of 5 divisions magnitude (in order to compute the photodiode shot-noise) [vii]. Since the electrical noise in the oscilloscope is roughly proportional to the caliber, it is always superior to the photodiode shot-noise. The amplifier noise becomes predominant only for weak signals. The noise spectral density has to be considered, since in bipolar transistor devices, such as amplifiers and oscilloscopes, it is generally not constant. On the other hand, since non-stationary noise, e.g., shot-noise, can be neglected with respect to the other noise sources, the overall noise can be assumed stationary.

We analyzed the variance, σ^2, of the cross-correlation time-of-arrival estimator in presence of additive gaussian noise [vii]. The ranging precision, i.e., standard deviation, can be put into form

$$\sigma \approx \frac{K}{SNR}$$

where $SNR = \frac{a}{\sigma_n}$ is the signal-to-noise ratio, σ_n^2 the noise variance, a the magnitude of the measured pulses, and K a waveform dependent parameter [vii]. Parameter K can be related to the rise time and fall time of the impulse-response of the detection stage. Thus, for a typical value of K=0.3 m, an SNR of 100 yields a ranging accuracy of 3 mm, independently of other error sources.

E. Temporal jitters

Time-of-arrival uncertainty of single photons is a fundamental temporal limitation. But, in our system, the detected laser pulse contains typically 10^4 photons, this effect can thus be neglected. On the other hand, the digital signal is affected by a temporal uncertainty with respect to the sampling grid of the oscilloscope. We evaluated this uncertainty, which is also an estimate of the sampling clock stability, to be at a few picoseconds level, over a typical 10 μsec interval. It can, therefore, be neglected. In order to analyze the effect of the signal sampling, we performed numerical simulations. A careful modeling of the instrumentation yielded a dispersion of 20 psec (3 mm).

F. Budget of error sources

Error source	Type	Order of magnitude	Conditioning parameters
1. ATMOSPHERE			
Mean refraction correction	systematic	< 1 mm, 1 °C deviation	Micro-meteorological effects
Pathlength fluctuations	random	0.8 mm, $C_n^2 = 10^{-14}$ $m^{-2/3}$	Turbulence structure constant, C_n^2
Scintillation	random	shot-to-shot SNR fluctuations	C_n^2 and SNR
2. LASER			
Wavefront distortion	systematic	< 1 cm, 100 psec FWHM laser	Cavity mode build-up

3. RECEIVER			
Electronic noise	random	3 mm, SNR=100	K, SNR
Magnitude related biases in the amplifier	systematic	negligible, after numerical correction	Correction model
Sampled signal aliasing	random	< 3 mm, 1 nsec sampling	sampling period, detection response-time
4. WIDE-ANGLE RANGING			
Pulse superimposition	systematic	negligible, when using deconvolution estimator and proper data sorting	Reference-pulse waveform, instrumental pulse discrimination

Table 2 : Summary of error sources limiting the ranging accuracy

Table 2 summarizes the accuracy limitation from the error sources described in the previous sub sections. We can assume from this analysis that cm accuracy is achievable with the current system. In the next section we present an experimental verification of this assumption.

V. RANGING PERFORMANCE EVALUATION FROM TERRESTRIAL EXPERIMENTS

In order to assess for the ranging accuracy of the developed instrument we performed three terrestrial experiments, differing by pathlength, instrumental configurations and turbulence regimes. For each experiment, we evaluated the standard deviation for relative range estimations and compared it to the theoretical precision, predicted by the above equation of σ. The theoretical precision gives an estimate of the single-shot accuracy of a sequence of measurements, characterized by its accuracy-constant K, and its SNR. Since standard deviations do not reveal biases in relative-distances, we also performed repeatability tests. Therefore, we computed mean relative distances and error bars for several samples of 100 measurements. Discrepancies between mean relative distances and error bars, with respect to the overall mean value, were used as an indicator of biases. The results and main characteristics of these experiments have been presented in [vii]. We summarize then in Table 3.

The first experiment validated the proposed instrument, composed of a mode-locked laser with a low impulse-response photodetector, and cross-correlation as time-of-arrival estimator. The standard deviation of relative distances, defined as single-shot accuracy, was better than 8 mm (SNR around 30). Biases, estimated by means of the above-mentioned repeatability test, were about 4 mm (SNR around 30). The second experiment showed that, when employing a transimpedance amplifier, the instrument still achieves centimeter precision, even for very low SNRs (e.g., 5.4 cm for SNR=5). The third experiment confirmed these performances at even longer distances, up to 1 km. Note that in the last experiment a diverging lens was used to achieve the beam divergence.

Exp.	Number of meas./seq.	SNR	K (m)	standard deviation σ_ρ (mm)	repeatability $\Delta\rho$ (mm)
1	43 - 100	33 - 91	0.16 - 0.29	3.6 - 7.8	< +/- 4.0
2	23 - 70	5 - 62	0.24	4.6 - 54	
3	6 - 25	15 - 36	0.72	22 - 60	< +/- 20

Table 3 : Summary of the main characteristics of three terrestrial experiments and the achieved accuracy (standard deviation and repeatability).

Figure 3 illustrates the relationship between single-shot accuracy and SNR, from data of the three terrestrial experiments. One can note that good agreement is found between measured and predicted values, even for high SNRs. This is due to the fact that amplifier biases are properly corrected. This is a fundamental assumption. Moreover, in these experiments the pulse shape

control and noise spectral distribution were identified as critical to keep low values of K and thus high ranging precision.

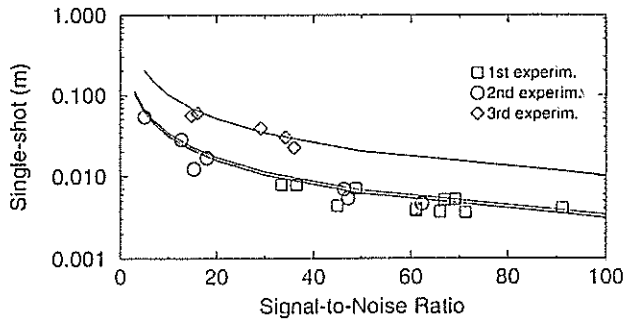

Figure 3 : Comparison of measured and predicted single-shot precision, versus SNR, for three terrestrial experiments. Note that, for K = *0.22 m, SNRs above 5 produce a 7 cm single-shot precision.*

In fact, the second experiment of Figure 3 was intended to test the performance of the inverse method of our multilateration technique from real data. It was implemented as a reduction of a typical aerial configuration to a two-dimensional terrestrial configuration. This experiment was conducted near Paris, in December 1995. After computation of the experimental range data, we found a relative positioning accuracy between 1 and 4.4 mm, rms, on the radial component, and between 1.8 cm and 7.8 cm on the transverse component [xv].These results are compatible with theoretical predictions from the covariance matrix and with numerical simulations, validating thus both the instrumentation and the simulation models. On the basis of these results, an aerial experiment simulation showed that the vertical component of retroreflectors could be estimated with a sub-mm accuracy, providing the instrumentation was adapted to the longer range constraint. An optimization of the present system is therefore proposed below.

VI. SYSTEM OPTIMIZATION

A. Aerial configuration

In a typical aerial configuration, i.e. 10 km altitude, the current instrumentation yields a SNR of 1.3 and a single-shot ranging accuracy of 21 cm. In order to satisfy the requirement of at least 3 cm ranging accuracy, we have to optimize the current instrumentation. This can be achieved by means of minimizing σ^2. As a first approach three different, though related, parameters can be considered. The first is the signal strength. Optimization could thus be achieved by maximizing the link budget (through the receiver surface or responsitivity), or the amplifier gain, or by reducing the response-time of the detection stage. The second is the overall electronic noise. Since it stems mostly from amplifier, this element should be optimized, e.g., by reducing the bandwidth. The third parameter is K. It can be lowered by reducing the response-time of the photodetector. When expressing σ^2 as a function of instrumental parameters, we identified the fundamental and independent parameters conditioning the ranging accuracy as being : amplifier gain, photodetector surface, and photodetector transit time. A further parameter can be investigated : the detector technology (APD vs. PIN photodiode).

1. Amplifier gain

Assuming the predominant noise source is the transimpedance amplifier, the SNR varies as the square-root of the gain, i.e., feed-back resistance. By taking into account the convolution effect of the impulse-response, for high gain, i.e., low bandwidth, the response is inversely

proportional to the gain, the accuracy is thus reduced. Identically, for low gain, i.e. high bandwidth, the fall-time of the impulse-response becomes independent of gain. The accuracy is therefore also reduced. An optimum gain near 1400 ohms can be found (see Figure 4), but the accuracy improvement is small. On must thus conclude that the amplifier gain can hardly be optimized.

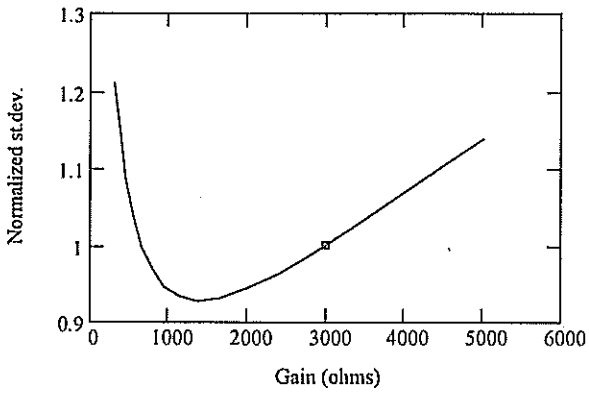

Figure 4 : Normalized accuracy (with respect to the current instrumentation, shown by the small box) vs. gain of the transimpedance amplifier

2. Photodetector surface

The photodetector surface must be high so as to keep an acceptable figure for the link budget with large field optics. But an increase of this surface produces an increase of the junction capacitance and, consequently, a reduction of the bandwidth. Finally, the accuracy becomes independent of the photodetector surface, for high values. Conversely, for low values the junction capacitance is no more a limiting parameter. Decreasing the surface just decreases the link budget and, therefore, the ranging accuracy. Hence, this parameter does not exhibit an optimum like the previous one (see Figure 5). A nearly asymptotic accuracy optimum could be achieved with a 10 cm^2 photosensitive surface detector. But this requirement seems rather unrealistic. Photodetector surface can, therefore, hardly be optimized.

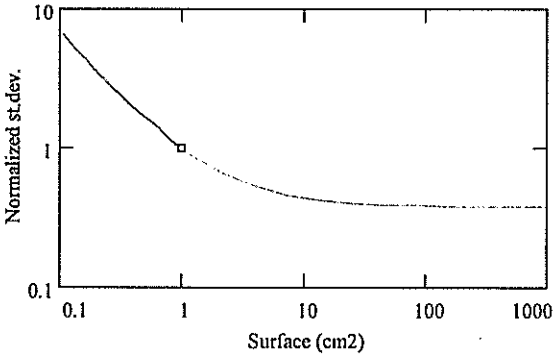

Figure 5 : Normalized accuracy vs. photodetector surface.

3. Photodetector transit time

Reduction of the photodetector transit time can be achieved, on a technological point of view, by reducing the width of the intrinseque zone (for a PIN structure). But the quantum efficiency is then consequently reduced. Again, this parameter does not exhibit any optimum and can hardly be improved (see Figure 6). But, once again, the current system is already near the optimum.

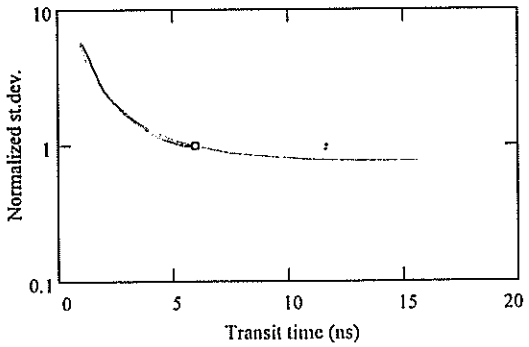

Figure 6 : Normalized accuracy vs. photodetector transit time.

4. Photodetector technology

Finally, there is an other fundamental parameter that we did not consider in the above optimization : the photodetector technology. The absorption coefficient of Si (of which the current PIN photodiode is made) is of 21 cm^{-1} at 1.064 µm whereas for Ge, it is about 10^4 cm^{-1} . But this latter technology is known as producing stronger electronic noise [xvi]. For InGaAs, sensitivities of 0.7 A/W are possible at 1.064 µm, but it seems that available detectors are limited to nearly 3 mm diameters. Actually, the best way to improve the current instrumentation seems to be the use of large photosensitive surface APDs. Such devices, with diameters up to 16 mm, are proposed by Advanced Photonix, for example. With a moderate avalanche gain of 100, a single-shot ranging accuracy of 1 cm should be achievable for an aerial configuration at 10 km altitude.

B. Spatial configuration

On the other hand, a spaceborne system would need a more fundamental revision of the instrumentation. To meet higher altitude requirements, the use of a telescope seems necessary and possible since, for the same network areas, the field of view is now much narrower, e.g., 0.01 rad. Velocity aberration correction can be achieved by the use of spoiled cube corners, but with a loss in the link budget amounting to a factor of 36. In order to achieve centimeter ranging accuracy, the instrumentation should be based on a 30 cm telescope, 1 J laser, 10 cm retroreflectors, 5 mm diameter APD of 10 A/W responsitivity, and 10,000 gain transimpedance amplifier. Actually, the single-shot ranging accuracy would then be between 2.3 cm and 5.3 cm from center to the half-width of the laser beam. A rough pointing system would also be necessary, in order to acquire data from an extended part of the orbit.

In this configuration, atmospheric effects are slightly different. On the transmission point of view, cirrus clouds have to be taken into account. Like for all spaceborne optical applications, cloud cover is a main limitation to the feasibility of surveys. Operational parameters, such as laser repetition frequency and spatial reflector density, have therefore to be carefully chosen in order to achieve the desired positioning accuracy from a single satellite passage. Concerning turbulence aspects, the dynamic layer is now located far away from the laser source. The main consequence on the link budget is that beam spreading and scintillation are stronger. For the same reasons, the pdf of scintillation becomes exponential, i.e., with unity intensity contrast. The effects of these error sources are still under investigation. But since the instrumental models have now been validated experimentally, they can be applied in numerical simulations of aerial and spatial configurations of the proposed positioning technique.

VII. CONCLUSION

A wide-angle laser ranging system, intended to achieve a new geodesy technique based on aerial or spatial multilateration, has been presented. A first instrumentation has been fully

validated on several terrestrial experiments. Results are compatible with theoretical predictions, related to the electrical SNR. An optimization for airborne experiments of the current instrument has been proposed. It consists mainly on replacing the PIN photodiode by a large aperture APD. This solution is now under investigation, with the aim of conducting an airborne experiment during 1997. From link budget considerations, an extension to a future spaceborne configuration seems also possible. But therefore, a more classical instrumentation, using a telescope, would be necessary.

ACKNOWLEDGMENTS

The authors would like to thank F. Pierron and his team of the Mobile Satellite Laser Station, Côte d'Azur Observatory, Grasse, France, for having made possible the experimentation with their mode-locked laser. They would also like to acknowledge Dr. J. Pelon, as well as D. Bruneau, of the Service d'Aéronomie, CNRS, Paris, France, for their contributions in meteorological aspects and advises in laser instrumentation, respectively.

REFERENCES

[i] M. Kasser and IGN, "Method for determining the spatial coordinates of points, applications of said method to high prescision topography, system and optical device for carrying out said method", US Patent 774,038, 1991

[ii] O. Bock, C. Thom, M. Kasser and D. Fourmaintraux : Development of a new airborne laser subsidence measurement system, aiming at mm-accuracy, Proceedings of the Fifth International Symposium on Land Subsidence (FISOLS-95), The Hague 16-20 October 1995, Balkema Publisher

[iii] D. Fourmaintraux, M. Flouzat, M.J. Bouteca, M. Kasser, (1994) Improved subsidence monitoring methods. SPE, paper 28095, Int. Symp. SPE-ISRM Eurock'94, Balkema Publisher

[iv] W. D. Kahn, J. J. Degnan and T. S. Englar, Jr : The airborne Laser Ranging System, Its Capabilities and Applications, Nasa Tech. Memo. 83984, Sept. 1982, Goddard Space Flight Center, Greenbelt, Maryland

[v] H. Lutz, W. Krause and G. Barthel : High-Precision Two-Colour Spaceborne Laser Ranging System for Monitoring Geodynamic Processes, 33rd Congress of the International Astronautical Federation, Paris, France, September 1982

[vi] S. C. Cohen, J. J. Degnan, J. L. Bufton, J. B. Garvin, J. B. Abshire : The Geoscience Laser Altimetry/Ranging System, IEEE Tr. on Geoscience and Remote Sensing, Vol. GE 25, No. 5, Sept. 1987

[vii] O. Bock, Ch. Thom, M. Kasser & J. Pelon, Ranging Performance Evaluation of the Wide-Angle Laser Ranging System, IEEE Tr. on Geoscience and Remote Sensing, to be published

[viii] J. J. Degnan : Millimeter Accuracy Laser Ranging : A Review, Geodynamics Serie volume 25, Contributions of Space Geodesy to Geodynamics: Technology, American Geophysical Union, 1993

[ix] J. W. Marini and C. W. Murray : Correction of laser range tracking data for atmospheric refraction at elevation angles above 10 degrees, GSFC, Nasa Technical Memo, Nov. 1973

[x] V. I. Tatarskii : Wave propagation in a turbulent medium, (translated by R.A. Silverman) McGraw-Hill, New-York 1961

[xi] M. E. Gracheva, A. S. Gurvich, S. S. Kashkarov and VI. V. Pokasov : Similarity Relations and Their Experimental Verification for Strong Intensity Fluctuations of Laser Radiation, Topics in Applied Physics, Vol. 25 : Laser Beam Propagation in the Atmosphere, Ed. J. W. Strohbehn, Springer-Verlag, 1978

[xii] J. W. Strohbehn : Modern Theories in the Propagation of Optical Waves in a Turbulent Medium, Topics in Applied Physics, Vol. 25, Laser Beam Propagation in the Atmosphere, Ed. J.W. Strohbehn, Springer-Verlag, 1978

[xiii] J. J. Degnan : Satellite Laser Ranging : Current Status and Future Prospects, IEEE Tr. on Geoscience and Remote Sensing, Vol. GE-23, No. 4, July 1985

[xiv] V. Kubecek, K. Hamal, I. Prochazka, R. Buzelis, A. Dement'ev, Optics Commun., Vol. 73, No. 3, 1989

[xv] O. Bock, M. Kasser Ch. Thom, & J. Pelon, "Precise Relative Positioning by Wide - Angle Laser Ranging", submitted to IEEE Tr. on Geoscience and Remote Sensing

[xvi] H. Melchior : Demodulation and photodetection techniques, Laser Handbook, Ed. F.T. Arecchi & E.O. Schultz-Dubois, North-Jolland Publishing Company, Amsterdam, 1972.